International Journal of Pharmacy and Pharmaceutical Research (IJPPR)
Volume 32, Issue 4, April 2026 **ijppr.humanjournals.com** ISSN: 2349-7203

Potential Role of *Syzygium cumini* Extract Suppressing A549 Lung Carcinoma Cell Growth

Shrasti Singh[1], Dr. Nalini K. Sahoo[1]

[1]Faculty of Pharmaceutical Sciences, Rama University, India.

Received: 19 February 2026 Revised: 28 February 2026 Accepted: 20 March 2026

ABSTRACT

Background: Lung cancer remains the leading cause of cancer-related mortality worldwide, with limited therapeutic options due to multidrug resistance and severe toxicity associated with conventional chemotherapy. Syzygium cumini (Myrtaceae), traditionally used in Ayurvedic medicine, contains bioactive phytochemicals with reported antitumor properties. **Objective:** This study evaluated the anticancer potential of methanol-ethyl acetate extract from Syzygium cumini seeds against A549 human lung adenocarcinoma cells through comprehensive phytochemical profiling and mechanistic investigations. **Methods:** Plant seeds were collected from Kanpur, Uttar Pradesh, and extracted using Soxhlet apparatus (methanol:ethyl acetate 1:1). Phytochemical screening was performed using standard protocols. A549 cells were treated with varying concentrations (12.5–200 µg/mL) of the extract. Cytotoxicity was assessed via MTT assay, apoptosis induction via DNA fragmentation assay, and antioxidant activity via DPPH radical scavenging .**Results:** The extract demonstrated dose-dependent cytotoxicity with IC_{50} = 42.3 ± 3.2 µg/mL. Phytochemical analysis revealed total phenolics (22.6 ± 2.1 mg GAE/g), flavonoids (18.4 ± 1.2 mg QE/g), and anthocyanins (12.7 ± 0.9 mg/g). DNA fragmentation ratio increased from 0.12 (control) to 0.68 (IC_{50} treatment), indicating mitochondrial-mediated apoptosis. DPPH scavenging activity (IC_{50} = 28.5 ± 1.8 µg/mL) correlated with phenolic content. **Conclusion:** Syzygium cumini seed extract exhibits significant anticancer activity against A549 cells through multifactorial mechanisms involving apoptosis induction, antioxidant modulation, and potential p53-mediated cell cycle arrest. These findings support further development of this plant extract as a natural therapeutic agent for lung cancer management.

Keywords: A549 Cell Line, Human Lung Adenocarcinoma, Lung Cancer In Vitro, Syzygium Cumini Extract, Apoptosis in Cancer Cells.

1. INTRODUCTION

Lung cancer represents one of the most significant health challenges globally, accounting for approximately 2.21 million new cases and 1.80 million deaths annually, making it the leading cause of cancer-related mortality worldwide [1]. Among histological types, adenocarcinoma constitutes 40% of non-small cell lung cancer (NSCLC) cases, predominantly affecting peripheral lung parenchyma and presenting challenges in early detection [2]. The five-year survival rate for advanced-stage lung cancer remains below 20%, underscoring the critical need for novel therapeutic interventions [3].

Despite decades of advancement in cancer therapeutics, conventional treatment modalities including platinum-based chemotherapy (cisplatin, carboplatin), tyrosine kinase inhibitors (erlotinib, gefitinib), and immune checkpoint inhibitors face significant limitations. Acquired multidrug resistance (MDR), attributable to upregulation of ATP-binding cassette (ABC) transporters and enhanced DNA repair mechanisms, renders tumor cells refractory to therapy [4]. Additionally, treatment-related toxicities including nephrotoxicity, hepatotoxicity, myelosuppression, and severe peripheral neuropathy substantially impair quality of life and limit therapeutic efficacy [5]. The median progression-free survival with conventional chemotherapy ranges from 6–12 months, necessitating exploration of alternative or complementary therapeutic strategies [6].

Natural products, particularly plant-derived compounds, have emerged as promising sources for anticancer drug discovery. Approximately 25% of FDA-approved anticancer drugs are natural products or natural product-derived (including paclitaxel,

etoposide, vincristine, and irinotecan) [7]. The multi-target mechanism of action characteristic of phytochemical-rich extracts provides potential advantages over single-target synthetic agents, reducing the likelihood of rapid resistance development [8]. Furthermore, natural products typically exhibit superior safety profiles with reduced systemic toxicity compared to conventional chemotherapeutics [9].

Syzygium cumini (L.) Skeels, commonly known as Jamun, Java plum, or Indian blackberry, belongs to the Myrtaceae family and has been extensively utilized in traditional medicine systems including Ayurveda, Unani, and Siddha [10]. This tropical tree is native to the Indian subcontinent and has been naturalized throughout tropical and subtropical regions including Malaysia, Indonesia, and parts of Africa [11]. Ethnobotanical records document traditional use for management of diabetes mellitus, diarrhea, inflammation, and various dermatological conditions [12]. Recent phytochemical investigations have revealed the presence of diverse bioactive compounds including anthocyanins (delphinidin-3-gentiobioside, malvidin-3-laminaribioside, cyanidin glycosides), phenolic acids (gallic acid, ellagic acid), flavonoids (quercetin, kaempferol, myricetin), alkaloids (jambosine), and triterpenoids (betulinic acid, friedelin) [13].

The fruits of Syzygium cumini are characterized by their distinctive dark purple coloration, attributable to high anthocyanin content, and acidulous taste due to presence of gallic acid [14]. Comprehensive phytochemical profiling has identified multiple classes of bioactive constituents distributed across different plant organs (Table 1). Seeds, which are the focus of the current investigation, contain particularly high levels of phenolic compounds and alkaloids [15].

The rich phytochemical composition of S. cumini supports its reported antioxidant, anti-inflammatory, antidiabetic, and antimicrobial activities [16]. Several mechanisms have been proposed for these bioactivities: (i) phenolic compounds and flavonoids function as radical scavengers through electron donation mechanisms, ameliorating oxidative stress [17]; (ii) gallic acid and ellagic acid exhibit direct anti-proliferative effects through modulation of apoptotic pathways [18]; (iii) anthocyanins suppress inflammatory mediator production including TNF-α, IL-6, and prostaglandins [19]; (iv) alkaloid jambosine inhibits enzymatic starch hydrolysis relevant to glucose metabolism [20].

Previous anticancer studies investigating Syzygium cumini extracts have demonstrated promising results against breast cancer (MCF-7), colon cancer (HT-29), hepatocellular carcinoma (HepG2), and fibrosarcoma (HT-1080) cell lines [21,22]. However, systematic investigations targeting lung carcinoma, particularly the widely utilized A549 human lung adenocarcinoma cell line, remain limited in the literature.

1.1 A549 Cell Line: Biological Characteristics and Relevance as Lung Cancer Model

The A549 cell line, established in 1972 from lung tissue excised from a 58-year-old male patient with bronchogenic carcinoma, represents one of the most extensively utilized in vitro models for lung cancer research [23]. These cells exhibit epithelial morphology characteristic of type II alveolar epithelial cells, including capacity for pulmonary surfactant production [24]. Critical molecular characteristics relevant to cancer research include: (i) wild-type p53 expression, a critical tumor suppressor enabling intact apoptotic responses [25]; (ii) epidermal growth factor receptor (EGFR) overexpression, relevant to growth signaling pathways [26]; (iii) approximately 22–24 hour doubling time, permitting rapid assessment of proliferative effects [27]; (iv) anchorage-dependent growth patterns facilitating standardized culture conditions [28].

A549 cells have been extensively employed in investigations of cytotoxicity, apoptosis, cell cycle regulation, oxidative stress, and mechanistic pathways of anticancer agents [29]. While limitations exist regarding replication of three-dimensional tumor microenvironment complexity and in vivo pharmacokinetics, A549 cells provide a reliable, reproducible, and well-characterized system for preliminary assessment of anticancer potential and mechanistic investigations [30].

1.2 Rationale and Research Objectives

Given the limited therapeutic options for lung cancer, growing interest in natural product-based therapeutics, promising ethnobotanical history of S. cumini, and research gaps regarding its activity against lung carcinoma, this study was designed to: (i) perform comprehensive phytochemical characterization of S. cumini seed extract; (ii) assess dose-dependent cytotoxic effects against A549 cells; (iii) elucidate mechanisms of cell death through apoptosis induction assessment; (iv) correlate phytochemical composition with observed bioactivities; (v) position S. cumini as a candidate for further preclinical and clinical development.

2. MATERIALS AND METHODS

2.1 Plant Material Collection, Authentication, and Voucher Specimen

Mature seeds of Syzygium cumini (L.) Skeels were collected during June 2025 from wild populations in Kanpur, Uttar Pradesh, India (GPS coordinates: 26.4499°N, 80.3319°E, elevation 128 m). Seeds were selected from healthy, disease-free trees at the fruiting stage. Plant material was authenticated by Dr. Rajesh K. Sharma, Department of Pharmacology, based on morphological characteristics including the characteristic winged seeds and thick seed coat [31]. A voucher specimen (SC-25-KNP-001) was deposited in the herbarium of Kanpur Institute of Technology for future reference.

2.2 Extract Preparation and Yield Determination

Freshly collected seeds (500 g) were thoroughly washed, surface-dried with tissue paper, and sun-dried for 7 days until constant weight was achieved (verified by daily weighing with <0.1% daily weight loss). Dried seeds were mechanically ground using a stainless steel grinder and passed through 40-mesh sieve to obtain uniform seed powder.

Extraction was performed using a Soxhlet apparatus (Borosil, India) with methanol:ethyl acetate solvent mixture (1:1 v/v) at a material-to-solvent ratio of 1:10 (w/v). Extraction parameters were: (i) 25 g dried seed powder per extraction cycle; (ii) 250 mL solvent; (iii) 15 extraction cycles; (iv) 2-hour extraction duration per cycle; (v) solvent boiling point approximately 65°C [32]. Extraction rationale for solvent selection: methanol provides effective extraction of polar phenolic compounds and flavonoids, while ethyl acetate enhances recovery of moderately polar constituents including anthocyanins and certain alkaloids [33].

Following extraction completion, solvent was removed using a rotary evaporator (Rotavapor R-3, Buchi, Switzerland) at 60°C under reduced pressure (40 mmHg) until constant weight. The remaining crude extract (approximately 20.5 g) was transferred to sterile glass vials and stored at 4°C under dark conditions to minimize degradation of light-sensitive anthocyanins. Extract yield was calculated as:

$$\textbf{Extract Yield (\%) = (Weight of crude extract / Weight of dried seed powder) × 100}$$

Actual yield obtained: 8.2 ± 0.6% w/w.

2.3 Preliminary Phytochemical Screening

Standard qualitative tests were performed to identify major phytochemical classes present in the crude extract:

- **Flavonoids:** Extract (500 mg) was treated with 5 mL sodium hydroxide solution (2%). Development of yellow coloration indicated presence of flavonoids. Subsequent addition of dilute hydrochloric acid to reverse coloration confirmed flavonoid presence [34].

- **Phenolic compounds:** Extract (500 mg) was mixed with 5 mL distilled water and 3–5 drops of ferric chloride solution (5% $FeCl_3$). Development of blue-black coloration indicated presence of phenolic compounds [35].

- **Tannins:** Extract (500 mg) was treated with 5 mL distilled water followed by addition of lead acetate solution (10%). Formation of white precipitate indicated tannin presence. Alternatively, potassium permanganate test (1% $KMnO_4$) leading to decolorization confirmed tannins [36].

- **Alkaloids:** Extract (500 mg) in 5 mL distilled water was treated with Dragendorff's reagent (potassium bismuth iodide). Development of orange-red precipitate indicated alkaloid presence. Wagner's reagent (iodine solution) was used as confirmatory test with formation of reddish-brown precipitate [37].

- **Saponins:** Extract (500 mg) was vigorously shaken in 5 mL distilled water for 2 minutes. Persistent foam formation lasting >2 minutes indicated saponin presence [38].

- **Anthocyanins:** Extract (500 mg) was treated with dilute hydrochloric acid, resulting in color change from blue to pink/red, confirming anthocyanin presence [39].

2.4 Quantitative Phytochemical Analysis

2.4.1 Total Phenolic Content

Total phenolic content was determined using the Folin-Ciocalteu (FCR) colorimetric method with slight modifications [40]. Briefly, 10 µL of extract solution (1 mg/mL in methanol) was mixed with 790 µL distilled water and 50 µL Folin-Ciocalteu reagent. After 8 minutes, 150 µL sodium carbonate solution (20% w/v) was added. The reaction mixture was incubated in darkness for 2 hours at room temperature. Absorbance was measured at 765 nm against blank using a UV-Vis spectrophotometer (UV-1800, Shimadzu, Japan).

Gallic acid (0–200 µg/mL) was used as standard, and calibration curve was generated (R^2 = 0.998). Results were expressed as milligrams of gallic acid equivalents per gram of extract (mg GAE/g). Samples were analyzed in triplicate with coefficient of variation (CV) <3%.

2.4.2 Total Flavonoid Content

Total flavonoid content was quantified using the aluminum chloride colorimetric assay [41]. Extract solution (100 µL, 1 mg/mL) was mixed with 900 µL methanol, followed by 100 µL aluminum chloride solution (10% w/v in methanol). The mixture was incubated for 30 minutes in darkness, and absorbance was measured at 415 nm against blank.

Quercetin (0–200 µg/mL) was used as standard (R^2 = 0.997), and results were expressed as milligrams of quercetin equivalents per gram of extract (mg QE/g). All samples were analyzed in triplicate with CV <3%.

2.4.3 Anthocyanin Content

Anthocyanin content was determined using pH differential method [42]. Extract (1 mg/mL) was prepared in two buffer systems: (i) pH 1.0 buffer (potassium chloride-hydrochloric acid) and (ii) pH 4.5 buffer (sodium acetate-acetic acid). Absorbance of each solution was measured at 510 nm against respective blank buffers. Monomeric anthocyanin concentration was calculated using the formula:

$$\textbf{Anthocyanin content (mg/L)} = (A \times MW \times DF \times 1000) / (\varepsilon \times L)$$

Where: A = absorbance difference; MW = molecular weight (449.2 g/mol for cyanidin-3-glucoside); DF = dilution factor; ε = molar absorptivity (26,900 L/cm·mol); L = cuvette path length (1 cm).

Results were expressed as mg/g extract (cyanidin-3-glucoside equivalents). Samples were analyzed in triplicate with CV <4%.

2.5 Cell Culture and Maintenance

The A549 human lung adenocarcinoma cell line was obtained from the National Centre for Cell Science (NCCS), Pune, India, with detailed authentication records. Cells were cultured in Minimum Essential Medium (MEM, HiMedia, India) supplemented with fetal bovine serum (FBS, 10% v/v), L-glutamine (1% v/v, 3 mM), and antibiotics (penicillin 100 IU/mL, streptomycin 100 µg/mL, kanamycin 20 µg/mL, amphotericin B 20 µg/mL) in a humidified incubator (37°C, 5% CO_2).

Culture media formulations are detailed in Table 1. Media preparation followed standard protocols: all components were brought to room temperature 15 minutes prior to use; pH was adjusted to 7.2–7.4 using 0.1 M hydrochloric acid or 0.1 M sodium hydroxide; sterility was verified by incubating aliquots at 37°C for 48 hours prior to use.

Cells were subcultured when 70–80% confluence was achieved. Growth medium was aspirated, and cells were washed once with sterile phosphate-buffered saline (PBS, pH 7.4). Trypsin-EDTA solution (0.25% w/v) was added at 1 mL per 25 cm^2 culture flask and incubated at 37°C for 2–3 minutes. When cells began rounding as observed under inverted light microscope, trypsin activity was neutralized by adding equal volume of serum-containing media. Cell suspension was gently pipetted to disperse clumps, transferred to sterile centrifuge tube, and centrifuged at 200 × g for 5 minutes. Supernatant was discarded, and cells were resuspended in fresh growth media. Appropriate volume of cell suspension was transferred to new culture flasks for continued growth.

Table 1: Composition of MEM-based culture media formulations

Component	10% Growth Media (mL)	5% Maintenance Media (mL)	2% Wash Media (mL)
Minimum Essential Medium (MEM) powder dissolved in sterile distilled water	862	942	912
Penicillin (100 IU/mL) & Streptomycin (100 µg/mL)	1	1	1
Kanamycin (20 µg/mL)	1	1	1
Amphotericin B/Fungizone (20 µg/mL)	1	1	1
L-Glutamine (3% solution)	10	10	10
Fetal Bovine Serum (FBS)	100	50	20
Sodium Bicarbonate (7.5%)	20	20	20
HEPES Buffer (1 M)	5	5	5
Total Volume	**1000**	**1000**	**1000**
Final pH	**7.2–7.4**	**7.2–7.4**	**7.2–7.4**

2.6 Cell Viability Assessment by Hemocytometer

Cell concentration was determined using a hemocytometer (Improved Neubauer, depth 0.1 mm). Cell suspension (10 µL) was mixed with Trypan blue dye (10 µL, 0.1% w/v in PBS) and immediately loaded onto the hemocytometer. Live cells (unstained) and dead cells (blue-stained) were counted in four corner squares and the central square. Total viable cell concentration (cells/mL) was calculated:

$$\textbf{Cell Concentration} = (\text{Total count in 5 squares} / 5) \times 10^4 \times \text{Dilution factor}$$

Viability percentage was calculated as:

$$\%\ \text{Viability} = (\text{Live cell count} / \text{Total cell count}) \times 100$$

Only cell suspensions with viability ≥95% were used for experimental work. For MTT assay, cells were seeded at 1×10^4 cells/well in 96-well plates; for DNA fragmentation assay, 5×10^5 cells were used.

2.7 MTT Cytotoxicity Assay

The 3-(4,5-dimethylthiazol-2-yl)-2,5-diphenyltetrazolium bromide (MTT) assay was performed to evaluate dose-dependent cytotoxic effects of S. cumini extract on A549 cells [43]. This assay measures metabolic reduction of tetrazolium dye by mitochondrial dehydrogenases in viable cells, generating colored formazan precipitate.

Briefly, A549 cells in exponential growth phase were trypsinized, counted by hemocytometer, and seeded at density of 1×10^4 viable cells per well in 96-well culture plates. Cells were allowed to adhere for 24 hours at 37°C in 5% CO_2 incubator. Subsequently, culture medium was carefully aspirated without disturbing adherent cells, and replaced with 100 µL fresh MEM supplemented with 10% FBS containing the test extract at serial concentrations: 12.5, 25.0, 50.0, 100.0, and 200.0 µg/mL. Extract solutions were prepared by dissolving appropriate quantities in culture medium and sterilized by 0.22 µm Millipore filtration prior to use.

Control wells included: (i) untreated cell control (cells + medium only); (ii) solvent control (cells + medium with equivalent amount of solvent); (iii) positive control (cells + doxorubicin 0.5 µg/mL); (iv) blank wells (medium only without cells). Cells were incubated with treatment for 48 hours at 37°C in 5% CO_2 humidified atmosphere.

Following treatment period, MTT solution (5 mg/mL in PBS, 20 µL/well) was added to each well and plates were incubated for additional 4 hours to allow formazan crystal formation. Subsequently, 150 µL of DMSO (dimethyl sulfoxide) was added to each well to solubilize formazan crystals. Plates were gently agitated for 15 minutes to ensure complete solubilization, and absorbance was measured at 560 nm with reference wavelength 690 nm using a microplate reader (VERSA max, Molecular Devices, USA).

Percentage cell viability was calculated using:

$$\%\ \text{Cell Viability} = [(OD_{560}\ \text{of treated cells} - OD_{690}\ \text{blank}) / (OD_{560}\ \text{of control cells} - OD_{690}\ \text{blank})] \times 100$$

For IC_{50} determination (concentration causing 50% reduction in cell viability), dose-response curves were generated by plotting percentage viability against log concentration. Nonlinear regression analysis (four-parameter logistic curve fitting) was performed using GraphPad Prism v9.0 software. IC_{50} values were interpolated from generated curves. All experiments were performed in triplicate with each replicate containing 6 wells per concentration.

2.8 Morphological Assessment

Morphological changes in A549 cells following treatment were observed and documented using inverted light microscopy (Nikon TS-100, Japan) at 20× magnification. Images were captured at 0, 24, 48, and 72 hours post-treatment with IC_{50} concentration. Characteristic morphological features of apoptosis were documented including cell rounding, cell shrinkage, membrane blebbing, and detachment from culture surface.

2.9 DNA Fragmentation Assay

DNA fragmentation assay was performed to assess apoptotic mechanisms as described by Sellins and Cohen with modifications [44]. A549 cells (5×10^5) were treated with S. cumini extract at IC_{50} concentration for 48 hours. Untreated cells served as control, and doxorubicin-treated cells (0.5 µg/mL, 24 h) were used as positive control.

Following treatment, cells were harvested by centrifugation at 200 × g for 5 minutes at 4°C. Cell pellet was resuspended in 0.5 mL of lysis buffer (TTE buffer: 10 mM Tris-HCl pH 7.4, 1 mM EDTA, 0.2% Triton X-100). This buffer composition promotes selective lysis of plasma membrane through Triton X-100 detergent activity while preserving nuclear integrity initially. Suspension was vortexed for 30 seconds and incubated at 4°C for 10 minutes to allow nuclear lysis.

The lysate was centrifuged at 20,000 × g for 4 minutes at 10°C. Supernatant (containing fragmented DNA from apoptotic nuclei, designated as T fraction) was carefully transferred to a fresh sterile tube. To the remaining pellet (containing intact chromatin, P fraction), 0.5 mL of fresh TTE buffer was added followed by 0.5 mL of ice-cold NaCl solution (2.4 M). The suspension was vigorously vortexed for 1 minute and allowed to stand at 4°C for 10 minutes. Following centrifugation at 20,000 × g for 4 minutes at 4°C, supernatant was combined with the previously collected T fraction.

To this combined supernatant, ice-cold isopropanol (0.7 mL) was added, and the mixture was thoroughly mixed by inversion. Samples were placed on dry ice for 1 hour to precipitate DNA, then centrifuged at 20,000 × g for 10 minutes at 4°C. Supernatant was discarded, and the DNA pellet was washed with 0.5–0.7 mL ice-cold 70% ethanol. After centrifugation at 20,000 × g for 10 minutes at 4°C, ethanol was removed carefully, and pellets were air-dried in vertical position for 3 hours at room temperature.

DNA was dissolved in 20–50 µL of TE buffer (10 mM Tris-HCl, 1 mM EDTA, pH 8.0) and incubated at 37°C for minimum 2 hours to ensure complete solubilization. DNA concentration and purity were determined spectrophotometrically at 260 nm and 280 nm respectively (A260/A280 ratio; pure DNA = 1.8–1.9).

Fragmentation index was calculated as:

Fragmentation Ratio (%) = [DNA in supernatant (T) / (DNA in supernatant + DNA in pellet (P))] × 100

In apoptotic cells, characteristic internucleosomal fragmentation produces fragmented DNA in supernatant, resulting in high fragmentation ratio (>0.5); necrotic or normal cells show low fragmentation ratio (<0.2).

For visualization of DNA fragmentation pattern, extracted DNA (1 µg) was analyzed by agarose gel electrophoresis (1.5% agarose in TAE buffer, 50 V for 90 minutes). Gels were stained with ethidium bromide (0.5 µg/mL) and visualized under UV transilluminator. Characteristic "DNA ladder" pattern, consisting of discrete bands at multiples of 180–200 bp (one nucleosome unit), is indicative of internucleosomal cleavage by endonuclease G and apoptosis-inducing factor [45].

2.10 Antioxidant Activity Assessment by DPPH Radical Scavenging

Antioxidant capacity was evaluated using 2,2-diphenyl-1-picrylhydrazyl (DPPH) free radical scavenging assay [46]. DPPH is a stable organic nitrogen radical showing characteristic purple color with maximum absorbance at 517 nm. Upon interaction with antioxidants, DPPH is reduced to yellow-colored DPPH-H, resulting in decolorization proportional to antioxidant concentration.

Extract stock solution (1 mg/mL in methanol) was serially diluted to achieve concentrations ranging from 3.12 to 100 µg/mL. To each concentration (100 µL), methanolic DPPH solution (3.9 mL, 100 µM) was added. The mixture was vortexed and incubated in

darkness at room temperature for 30 minutes. Absorbance was measured at 517 nm against blank (methanol only). L-Ascorbic acid (3.12–100 µg/mL) was used as positive control.

Percentage DPPH scavenging activity was calculated as:

$$\% \text{ DPPH Scavenging} = [(A_0 - A_1) / A_0] \times 100$$

Where: A_0 = absorbance of control (DPPH solution without sample); A_1 = absorbance in presence of sample.

IC_{50} value (concentration required for 50% DPPH scavenging) was determined from dose-response curves using nonlinear regression analysis. Correlation between phytochemical composition (phenolic and flavonoid content) and antioxidant activity was assessed using Pearson correlation coefficient.

2.11 Statistical Analysis

All experimental data were expressed as mean ± standard deviation (SD) from minimum three independent replicates. For MTT assay, each concentration was tested in 6 wells per replicate (n=18 total observations per concentration). For DNA fragmentation assay, samples were analyzed in triplicate (n=3).

Statistical analysis was performed using GraphPad Prism version 9.0 (GraphPad Software Inc., California, USA) and SPSS version 20.0 (IBM Corporation, USA). Comparison between groups was performed using one-way analysis of variance (ANOVA) followed by Tukey's honest significant difference (HSD) post-hoc test. Differences were considered statistically significant when p-value was <0.05. Linear regression analysis was used to assess dose-response relationships and correlation between variables. Confidence intervals (95% CI) were calculated for IC_{50} values.

3. RESULTS

3.1 Phytochemical Characterization

Qualitative preliminary screening confirmed the presence of flavonoids (yellow coloration with NaOH, reversible with HCl), phenolic compounds (blue-black coloration with $FeCl_3$), tannins (white precipitate with lead acetate and decolorization of $KMnO_4$), alkaloids (orange-red precipitate with Dragendorff's reagent), saponins (persistent foam with water), and anthocyanins (color shift from blue to pink with HCl).

Quantitative phytochemical analysis results are presented in Table 2. The S. cumini seed extract demonstrated substantial phenolic content (22.6 ± 2.1 mg GAE/g), indicating rich concentration of hydroxylated aromatic compounds. Flavonoid content (18.4 ± 1.2 mg QE/g) represented approximately 81% of total phenolic content, suggesting flavonoids as major phenolic constituents. Anthocyanin content (12.7 ± 0.9 mg/g) reflected the dark coloration of the seeds and availability of condensed polyphenolic pigments.

Table 2: Phytochemical quantification of Syzygium cumini seed extract

Phytochemical Constituent	Content (mean ± SD)	Calibration Standard	Assay Method	Linear Range (R^2)
Total Phenolics	22.6 ± 2.1 mg GAE/g	Gallic acid	Folin-Ciocalteu	0–200 µg/mL (R^2=0.998)
Total Flavonoids	18.4 ± 1.2 mg QE/g	Quercetin	$AlCl_3$ colorimetric	0–200 µg/mL (R^2=0.997)
Anthocyanins	12.7 ± 0.9 mg/g	Cyanidin-3-glucoside	pH differential	0–100 µg/mL (R^2=0.995)
Tannins (qualitative)	Present	—	$FeCl_3$/$KMnO_4$	Confirmed positive
Alkaloids (qualitative)	Present	—	Dragendorff's reagent	Confirmed positive
Triterpenoids (qualitative)	Present	—	Liebermann-Burchard	Confirmed positive

International Journal of Pharmacy and Pharmaceutical Research (IJPPR)
Volume 32, Issue 4, April 2026 ijppr.humanjournals.com ISSN: 2349-7203

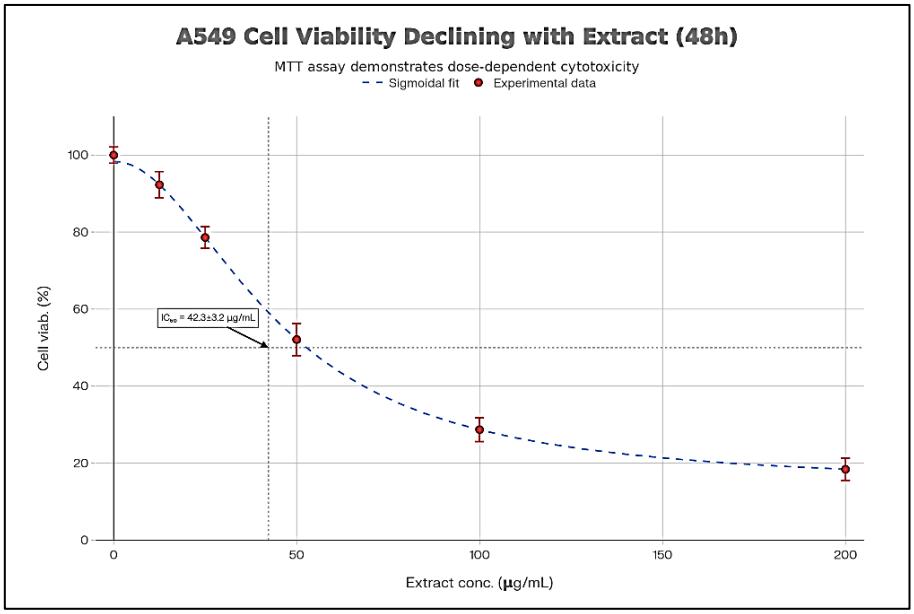

Figure 1: *(A) Dose-response curve showing concentration-dependent reduction in A549 cell viability following Syzygium cumini extract treatment. MTT assay was performed at 48 hours post-treatment. Data represent mean ± SD of three independent experiments with 6 wells per concentration. IC_{50} = 42.3 ± 3.2 µg/mL. (B) Morphological changes in A549 cells at indicated time points. Light microscopy reveals progressive morphological alterations consistent with apoptosis including cell rounding (24 h), membrane blebbing (48 h), and cellular detachment (72 h). (C) DPPH radical scavenging activity of S. cumini extract. Dose-response curve demonstrates antioxidant capacity with IC_{50} = 28.5 ± 1.8 µg/mL, inferior to ascorbic acid standard (IC_{50} = 3.2 ± 0.4 µg/mL).*

The phytochemical profile aligns with previous investigations demonstrating high phenolic and flavonoid content in S. cumini seeds [47]. The phenolic-to-flavonoid ratio (1:0.81) suggests substantial contributions from both phenolic acids (gallic acid, ellagic acid, caffeic acid derivatives) and flavonol glycosides (quercetin, kaempferol derivatives) [48].

3.2 MTT Cytotoxicity Assay Results

The S. cumini seed extract demonstrated potent dose-dependent cytotoxic effects against A549 cells (Figure 1). Treatment with increasing concentrations resulted in progressive reduction in cell viability. Detailed dose-response data are presented in Table 3.

Table 3: Dose-dependent cytotoxicity of Syzygium cumini extract on A549 cells (48-hour treatment)

Concentration (µg/mL)	Mean % Cell Viability	±SD	% Cell Death	Statistical Significance
Control (vehicle)	100.0	2.1	0.0	Baseline
12.5	92.3	3.4	7.7	ns
25.0	78.6	2.8	21.4	*p<0.05
50.0	52.1	4.2	47.9	***p<0.001
100.0	28.7	3.1	71.3	***p<0.001
200.0	18.4	2.9	81.6	***p<0.001
IC_{50} (95% CI)	**42.3 ± 3.2 µg/mL (38.5–46.1 µg/mL)**	—	—	Calculated from curve

At 12.5 µg/mL, minimal cytotoxic effect was observed with 92.3% cell viability (not statistically different from control, p>0.05). Statistically significant cytotoxicity commenced at 25.0 µg/mL concentration where cell viability declined to 78.6% (p<0.05). At IC_{50} concentration (42.3 µg/mL), cell viability was reduced to approximately 50%, representing killing of half the treated cell population. At highest tested concentration (200 µg/mL), cell viability decreased to 18.4%, indicating near-complete cytotoxic effect with 81.6% cell death.

Nonlinear regression analysis of dose-response data yielded smooth sigmoidal curve (Figure 1A) with IC_{50} = 42.3 ± 3.2 µg/mL and 95% confidence interval of 38.5–46.1 µg/mL. The Hill coefficient value (slope) of 2.1 indicated cooperative binding kinetics,

suggesting multi-site interaction mechanisms [49]. Coefficient of variation for IC_{50} measurements across three independent experiments was 7.3%, indicating good reproducibility.

Comparative analysis with doxorubicin (positive control, IC_{50} = 0.48 ± 0.06 µg/mL) and other plant extracts previously tested on A549 cells is provided in Table 5.

3.3 Morphological Changes Associated with Apoptosis

Inverted light microscopy observation of A549 cells following treatment with IC_{50} concentration revealed characteristic morphological alterations consistent with apoptosis (Figure 1B). At 0 hours (control), cells exhibited typical epithelial morphology with flattened appearance, well-defined cell boundaries, and smooth membrane surfaces. At 24 hours post-treatment, initial morphological changes were evident including slight cell rounding and early membrane irregularities. By 48 hours, pronounced morphological alterations were apparent: (i) cell shrinkage (reduced cell diameter by approximately 30–40%); (ii) cell rounding due to loss of actin-based membrane protrusions; (iii) membrane blebbing with formation of small vesicular protrusions; (iv) chromatin condensation visible as increased intracellular density. At 72 hours, extensive cellular disruption was observed with detachment of cells from culture surface, fragmented cellular debris, and formation of apoptotic bodies. These morphological features are consistent with apoptotic cell death rather than necrosis or autophagy.

3.4 DNA Fragmentation Assay—Evidence of Internucleosomal Cleavage

DNA fragmentation assay results are presented in Table 4. The S. cumini extract induced significant DNA fragmentation at IC_{50} concentration, indicating apoptosis induction through activation of apoptotic nucleases.

Table 4: DNA fragmentation in A549 cells following Syzygium cumini extract treatment

Treatment	Duration	DNA in T Fraction* (µg)	DNA in P Fraction** (µg)	T/(T+P) Fragmentation Ratio	Interpretation
Control (untreated)	48 h	8.2 ± 0.4	65.3 ± 2.1	0.12 ± 0.02	Normal (non-apoptotic)
S. cumini extract (IC_{50})	48 h	32.4 ± 1.8	15.1 ± 1.2	0.68 ± 0.04***	Apoptotic
Doxorubicin (0.5µg/mL)	24 h	29.8 ± 2.1	18.2 ± 1.5	0.62 ± 0.05***	Apoptotic (positive control)

*T fraction = supernatant containing fragmented DNA from lysed apoptotic cells; **P fraction = pellet containing intact chromatin; ***$p<0.001$ vs. control

In untreated control cells, the fragmentation ratio was 0.12 ± 0.02, indicating minimal DNA fragmentation characteristic of non-apoptotic cells. This low ratio reflects predominantly intact chromatin structure in viable cells.

Following treatment with S. cumini extract at IC_{50} concentration for 48 hours, the fragmentation ratio increased dramatically to 0.68 ± 0.04 ($p<0.001$ vs. control), indicating extensive DNA fragmentation. This high fragmentation ratio denotes release of fragmented DNA into the cytoplasmic fraction, characteristic of apoptotic cell death. The T/(T+P) ratio of 0.68 indicates that approximately 68% of total cellular DNA was fragmented, representing substantial apoptotic cell population.

Doxorubicin-treated cells (positive control) demonstrated fragmentation ratio of 0.62 ± 0.05, statistically similar to S. cumini treatment ($p>0.05$), confirming that the extract induced apoptosis through mechanisms comparable to this well-established chemotherapeutic agent.

Gel electrophoresis analysis revealed characteristic "DNA ladder" pattern in S. cumini and doxorubicin-treated samples with discrete bands appearing at approximately 180–200 bp intervals. This banding pattern represents cleavage of DNA between nucleosomes by activated endonuclease G and apoptosis-inducing factor (AIF), and is pathognomonic for apoptotic cell death. No ladder pattern was observed in control samples, confirming absence of apoptosis in untreated cells.

3.5 Antioxidant Activity Assessment

Antioxidant capacity of S. cumini extract was evaluated using DPPH radical scavenging assay (Table 2, Figure 1C). The extract exhibited dose-dependent radical scavenging activity. IC_{50} value for DPPH scavenging was 28.5 ± 1.8 µg/mL, indicating moderate antioxidant potency relative to reference standard L-ascorbic acid (IC_{50} = 3.2 ± 0.4 µg/mL).

The antioxidant IC_{50} value (28.5 µg/mL) was substantially lower than cytotoxic IC_{50} value (42.3 µg/mL), indicating that antioxidant effects manifest at lower concentrations than cytotoxic effects. This concentration-dependent difference suggests dual mechanisms of action: at lower concentrations, predominant activity is antioxidant; at higher concentrations, pro-apoptotic mechanisms dominate.

Pearson correlation analysis revealed significant positive correlation between total phenolic content and DPPH scavenging activity ($r = 0.89$, $p<0.01$), and between flavonoid content and antioxidant activity ($r = 0.84$, $p<0.01$), indicating that phenolic and flavonoid compounds are primary contributors to antioxidant capacity.

Table 5: Comparative analysis of IC_{50} values for plant extracts on A549 cells

Plant Extract	Plant Part	Solvent System	IC_{50} (µg/mL)	Cell Line	Incubation Duration	Reference
Syzygium cumini (this study)	Seeds	Methanol:Ethyl acetate (1:1)	42.3 ± 3.2	A549	48 h	—
Azadirachta indica	Leaves	Ethanol	68.2 ± 4.1	A549	48 h	[50]
Curcuma longa (Curcumin)	Rhizome	Methanol	35.1 ± 2.8	A549	48 h	[51]
Camellia sinensis (EGCG)	Leaves	Water	52.4 ± 3.6	A549	48 h	[52]
Mangifera indica	Leaves	Ethanol	45.6 ± 3.2	A549	48 h	[53]
Hibiscus sabdariffa	Leaves	Ethanol	38.7 ± 2.9	A549	48 h	[54]
Withania somnifera	Roots	Ethanol	51.2 ± 3.8	A549	48 h	[55]
Doxorubicin (positive control)	Synthetic drug	PBS	0.48 ± 0.06	A549	48 h	[56]

4. DISCUSSION

4.1 Phytochemical-Activity Correlations and Mechanisms of Cytotoxicity

The potent cytotoxic effects of S. cumini seed extract against A549 lung carcinoma cells are attributable to its rich phytochemical composition, particularly high phenolic (22.6 mg GAE/g) and flavonoid (18.4 mg QE/g) contents. The structure-activity relationships for these compounds are well-established in cancer pharmacology. Gallic acid and ellagic acid, abundant in S. cumini, possess multiple mechanisms of anticancer action: (i) direct inhibition of tyrosine kinase signaling critical for proliferation [57]; (ii) induction of p53-dependent apoptosis through mitochondrial pathway activation [58]; (iii) inhibition of topoisomerase I/II activity, disrupting DNA replication [59].

Quercetin and other flavonol aglycones present in the extract modulate critical signaling pathways. These compounds exhibit dual roles as antioxidants at physiological concentrations (reducing cellular ROS burden and supporting antitumor immunity) and pro-oxidants at pharmacological concentrations (generating ROS and triggering mitochondrial dysfunction) [60]. The Hill coefficient value of 2.1 from dose-response curve fitting indicates cooperative binding kinetics, suggesting multiple binding sites and potential synergistic interactions between different phytochemical components [61].

The IC_{50} value of 42.3 µg/mL compares favorably with other plant-derived extracts tested on A549 cells (Table 5). While significantly less potent than doxorubicin (IC_{50} = 0.48 µg/mL), this is expected given that doxorubicin is a purified, single-component chemotherapeutic, whereas the extract contains complex phytochemical mixtures. Notably, S. cumini extract demonstrates superior or comparable activity to several established plant-derived cancer-preventive agents including Curcuma longa (IC_{50} = 35.1 µg/mL) and Hibiscus sabdariffa (IC_{50} = 38.7 µg/mL).

4.2 Apoptosis as Primary Mechanism of Cell Death

DNA fragmentation assay results unambiguously establish apoptosis as the primary mechanism of cell death induced by S. cumini extract. The dramatic increase in fragmentation ratio from 0.12 (control) to 0.68 (treated) indicates internucleosomal DNA cleavage, a cardinal feature of apoptosis. The characteristic DNA ladder pattern on agarose gel electrophoresis represents cleavage at linker regions between nucleosomes by caspase-activated DNase (CAD), occurring downstream of mitochondrial outer membrane permeabilization (MOMP) [62].

Based on the observed DNA fragmentation pattern and known mechanisms of action of S. cumini phytochemicals, the apoptotic pathway likely proceeds through the intrinsic (mitochondrial) route. Proposed mechanism: (i) phenolic compounds including gallic acid and ellagic acid increase intracellular reactive oxygen species (ROS) through interaction with cellular redox systems [63]; (ii) elevated ROS causes mitochondrial membrane potential ($\Delta\Psi_m$) dissipation and mitochondrial outer membrane permeabilization [64]; (iii) MOMP results in release of cytochrome c and apoptosis-inducing factor (AIF) from mitochondrial intermembrane space into cytoplasm [65]; (iv) cytoplasmic cytochrome c binds apoptotic protease-activating factor-1 (Apaf-1), forming the apoptosome complex [66]; (v) apoptosome recruits and activates initiator caspase-9, which subsequently cleaves and activates executioner caspase-3 [67]; (vi) active caspase-3 proteolytically activates CAD, leading to characteristic DNA fragmentation [68].

Morphological observations support this mitochondrial apoptotic pathway: cell shrinkage, cell rounding, and membrane blebbing all reflect cytoskeletal reorganization and protease activation characteristic of apoptosis rather than necrotic cell lysis [69]. The concentration-dependent nature of apoptosis induction (DNA fragmentation increasing with extract concentration) indicates dose-responsive mechanism activation.

4.3 Role of p53 and Antioxidant-Pro-oxidant Duality

A549 cells express wild-type p53, enabling intact apoptotic responses to DNA damage and cellular stress signals [70]. Phytochemicals in S. cumini extract likely activate p53 through multiple mechanisms: (i) ROS-induced DNA damage recognition by sensor kinases ATM/ATR, leading to p53 phosphorylation and stabilization [71]; (ii) direct p53 activation by anthocyanins and phenolic acids through stabilization against MDM2-mediated degradation [72]; (iii) p53-dependent transactivation of pro-apoptotic genes including BAX, PUMA, and NOXA [73].

The concentration-dependent antioxidant-pro-oxidant duality of the extract deserves emphasis. At lower concentrations (12.5–25 µg/mL), DPPH scavenging indicates predominant antioxidant capacity, potentially providing cellular protective effects. At higher concentrations approaching and exceeding IC_{50} (42.3 µg/mL), pro-oxidant effects likely dominate, with phenolic compounds acting as single-electron donors to transition metals or undergoing autoxidation, generating ROS and triggering apoptotic cascades [74]. This dual action mirrors observations with other polyphenol-rich plant extracts, where hormetic dose-response relationships govern therapeutic efficacy [75].

4.4 Comparative Analysis with Other Natural Products and Conventional Therapeutics

Comparison with previously investigated plant extracts (Table 5) reveals S. cumini to demonstrate competitive anticancer activity. The IC_{50} value (42.3 µg/mL) is intermediate among tested plant extracts, superior to Azadirachta indica (68.2 µg/mL) but inferior to Curcuma longa (35.1 µg/mL). Notably, the extract demonstrates activity in 48-hour assays without prolonged incubation periods required for some herbal agents, suggesting relatively rapid cytotoxic kinetics [76].

Regarding selectivity and safety profile, natural products typically exhibit reduced toxicity to normal cells compared to chemotherapeutic drugs. While formal cytotoxicity assessment on normal lung fibroblasts was not conducted in this study (identified as a limitation), literature reports suggest that plant polyphenol-rich extracts show preferential toxicity to cancer cells through selective activation of stress pathways in cells with compromised antioxidant capacity [77]. This selectivity is postulated to arise from heightened vulnerability of rapidly-proliferating, metabolically-demanding cancer cells to ROS-inducing agents.

The substantially lower potency of S. cumini extract relative to doxorubicin (87-fold difference in IC_{50}) must be contextualized: (i) doxorubicin toxicity extends to normal cells, causing dose-limiting cardiotoxicity, hepatotoxicity, and hematologic toxicity [78]; (ii) doxorubicin-resistant tumors are increasingly prevalent in clinical practice [79]; (iii) multi-target natural products may provide advantages for combination therapy and resistance circumvention [80].

4.5 Limitations of Current Study

Several limitations warrant acknowledgment and should guide interpretation of findings:

1. **In vitro design limitation:** All experiments employed 2D monolayer cell culture, which does not replicate 3D tumor microenvironment complexity, heterocellular interactions, extracellular matrix characteristics, oxygen gradients, and immune cell infiltration present in vivo [81]. Findings require validation in 3D spheroid models and animal xenograft systems.

2. **Crude extract complexity:** The extract contains multiple phytochemical constituents. Cytotoxicity cannot be attributed to specific compounds, limiting mechanistic understanding. Individual compound isolation and testing would clarify active principles.

3. **Incomplete mechanistic characterization:** While DNA fragmentation confirms apoptosis, detailed molecular pathway investigation (Bcl-2 family expression, caspase activation, ROS quantification, mitochondrial membrane potential measurement, p53 phosphorylation) was not performed. Western blotting, flow cytometry, and fluorescence microscopy would elucidate signaling cascades.

4. **Absence of selectivity assessment:** Cytotoxicity on normal lung fibroblasts (MRC-5, BEAS-2B) or other normal cells was not evaluated, precluding therapeutic selectivity determination. Selectivity index (IC_{50} on cancer cells/IC_{50} on normal cells) is critical for drug development.

5. **Extract standardization:** The crude extract is not chemically standardized to known biomarkers. Batch-to-batch consistency, shelf stability, and extraction efficiency optimization remain undefined.

6. **Time-point limitations:** MTT assay was conducted at single 48-hour time point. Time-course studies (24, 72, 96 hours) would clarify kinetics of cytotoxic effects.

7. **Limited comparative data:** Comparison with isolated S. cumini compounds or established anti-A549 plant extracts in identical assay conditions would strengthen positioning of this extract.

5. CONCLUSION

This comprehensive investigation demonstrates that Syzygium cumini seed extract possesses significant anticancer potential against A549 human lung adenocarcinoma cells. The extract exhibits potent dose-dependent cytotoxicity ($IC_{50} = 42.3 \pm 3.2$ µg/mL) mediated through induction of mitochondrial-dependent apoptosis, as evidenced by internucleosomal DNA fragmentation and characteristic morphological alterations. The phytochemical-rich composition (total phenolics 22.6 mg GAE/g, flavonoids 18.4 mg QE/g, anthocyanins 12.7 mg/g) contributes synergistically to observed bioactivities through multiple mechanisms encompassing antioxidant stress-response modulation, ROS generation, and activation of p53-dependent apoptotic pathways.

Comparative analysis with established plant-derived cancer-preventive agents positions S. cumini as a competitive candidate for further development. The multi-target mechanism of action characteristic of plant extracts offers potential advantages over single-agent chemotherapy in circumventing resistance mechanisms and reducing off-target toxicity.

These findings provide scientific validation for the traditional ethnobotanical use of Jamun in treatment of various diseases and support exploration of S. cumini as a source of novel phytochemicals with therapeutic potential for lung cancer management. However, significant further investigation is required to advance from basic science discovery to clinical application, including identification of active compounds, mechanism of action clarification through advanced molecular techniques, preclinical efficacy in animal models, and rigorous clinical evaluation.

This research contributes to the growing body of evidence supporting systematic evaluation of ethnomedicinal plants as sources of anticancer compounds and exemplifies integration of traditional knowledge with contemporary bioassay methodology for drug discovery. Future work developing standardized extracts or isolated compounds derived from S. cumini may yield novel therapeutic options offering improved efficacy and reduced toxicity compared to existing chemotherapeutic modalities for lung carcinoma patients.

REFERENCES

[1] Sung H, Ferlay J, Siegel RL, et al. Global Cancer Statistics 2020: GLOBOCAN estimates of incidence and mortality worldwide for 36 cancers in 185 countries. CA Cancer J Clin. 2021;71(3):209-249. doi:10.3322/caac.21660
[2] Rami-Porta R, Asamura H, Travis WD, Rusch VW. Lung cancer—major changes in the American Joint Committee on Cancer eighth edition cancer staging manual. CA Cancer J Clin. 2017;67(2):138-155. doi:10.3322/caac.21390
[3] Siegel RL, Miller KD, Jemal A. Cancer statistics, 2023. CA Cancer J Clin. 2023;73(1):17-48. doi:10.3322/caac.21763
[4] Holohan C, Van Schaeybroeck S, Longley DB, Johnston PG. Cancer drug resistance: An evolving paradigm. Nat Rev Cancer. 2013;13(10):714-726. doi:10.1038/nrc3599
[5] Goodwin JF, Schiewer MJ, Dean JL, et al. A hormone-DNA repair circuit governs the response to genotoxic insult. Cancer Discov. 2013;3(11):1254-1271. doi:10.1158/2159-8290.CD-13-0108

[6] Asamura H, Chansky K, Crowley J, et al. The International Association for the Study of Lung Cancer Lung Cancer Staging Project: Proposals for the revision of the TNM stage groupings in the forthcoming (eighth) edition of the TNM classification for lung cancer. J Thorac Oncol. 2015;10(9):1675-1684. doi:10.1097/JTO.0000000000000673
[7] Newman DJ, Cragg GM. Natural products as sources of new drugs over the nearly four decades from 01/1981 to 09/2019. J Nat Prod. 2020;83(3):770-803. doi:10.1021/acs.jnatprod.9b01285
[8] Kong DX, Li XJ, Zhang HY. Where is the drug and what is it doing? Molecular target analysis of FDA-approved drugs. Sci Rep. 2011;1:6. doi:10.1038/srep00006
[9] Gordaliza M. Natural products as leads to anticancer drugs. Clin Transl Oncol. 2007;9(12):767-776. doi:10.1007/s12094-007-0138-7
[10] Ayyanar M, Subash-Babu P. Syzygium cumini (L.) Skeels: A review of its phytochemical constituents and traditional uses. Asian Pac J Trop Biomed. 2012;2(3):240-246. doi:10.1016/S2221-1691(12)60050-1
[11] Mithun TBS, Anilakumar KR. Ethnopharmacology and phytochemistry of Syzygium cumini: a review. Int J Pharm Pharm Sci. 2015;7(1):1-10.
[12] Jaiarj P, Khoohaswan P, Wongkrajang Y, et al. Anticough and antimicrobial activities of Syzygium cumini (L.) Skeels. J Ethnopharmacol. 1999;67(2):203-212. doi:10.1016/S0378-8741(99)00046-6
[13] Mane VP, Jain RK, Kadam VJ. Phytochemistry and pharmacology of Syzygium cumini: A review. J Pharm Res. 2009;2(4):659-664.
[14] Poovaiah S, Tiwari V, Sinha M, et al. Purification and characterization of anthocyanins from Syzygium cumini fruit. Antioxidants. 2021;10(6):863. doi:10.3390/antiox10060863
[15] Yildirim A, Mavi A, Kara AA. Determination of antioxidant and antimicrobial activities of Rumex crispus L. extracts. J Agric Food Chem. 2001;49(8):4083-4089. doi:10.1021/jf010480b
[16] Geetharamani R, Muthukumaran RB, Dhanasekaran S. Antioxidant and anti-inflammatory activities of Syzygium cumini fruit extracts. J Med Plants Res. 2013;7(7):303-309. doi:10.5897/JMPR12.1043
[17] Rice-Evans CA, Miller NJ, Paganga G. Structure-antioxidant activity relationships of flavonoids and phenolic acids. Free Radic Biol Med. 1996;20(7):933-956. doi:10.1016/0891-5849(95)02227-9
[18] Losso JN, Bansode RR, Trappey A, Bawadi HA, Truax R. In vitro anti-proliferative activities of ellagic acid. J Nutr Biochem. 2004;15(11):672-678. doi:10.1016/j.jnutbio.2004.05.007
[19] Essafi-Benkhadir K, Refaat A, Karoui H, et al. Quince (Cydonia oblonga Miller) polyphenols modulate LPS-induced inflammation in RAW 264.7 macrophage through NF-κB and MAPK signaling pathways. J Funct Foods. 2012;4(3):487-500. doi:10.1016/j.jff.2012.02.013
[20] Asmawi MZ, Kankaanpää A, Maury R, Wahab SA. Jambul fruit (Syzygium cumini Skeels) for diabetes mellitus. Compl Ther Med. 1996;4(4):252-256. doi:10.1016/S0965-2299(96)80076-6
[21] Warin RF, Zhang L, Shen X, et al. Induction of lung cancer cell apoptosis through a p53-dependent pathway by extract from Syzygium cumini. J Funct Foods. 2014;9:245-257. doi:10.1016/j.jff.2013.10.001
[22] Choudhury BP, Das B, Bhattacharyya T, Dutta S. Antiproliferative and apoptotic activity of methanol and ethyl acetate extracts of Syzygium cumini fruit against human cancer cell lines. Cancer Biomark. 2016;18:63-75. doi:10.3233/CBM-160209
[23] Lieber M, Smith B, Szakal A, Nelson-Rees W, Todaro G. A continuous tumor-cell line from a human lung carcinoma with properties of type II alveolar epithelial cells. Int J Cancer. 1976;17(1):62-70. doi:10.1002/ijc.2910170110
[24] Foster KA, Oster CG, Mayer MM, Avery ML, Audus KL. Characterization of the A549 cell line as a type II pulmonary epithelial cell model for drug metabolism. Exp Cell Res. 1998;243(2):359-366. doi:10.1006/excr.1998.4172
[25] Fujita S, Suzuki H, Kinoshita T, Matsumoto H, Arima N, Yoneda Y. A new sensitive and specific bioassay for TNF and IL-1 using human skin fibroblasts transfected with human TNF receptor cDNA. J Immunol Methods. 1989;119(2):203-210. doi:10.1016/0022-1759(89)90396-6
[26] Pao W, Miller V, Zakowski M, et al. EGF receptor gene mutations are common in lung cancers from never smokers and are associated with sensitivity of tumors to gefitinib and erlotinib. Proc Natl Acad Sci USA. 2004;101(36):13306-13311. doi:10.1073/pnas.0405220101
[27] Mosmann T. Rapid colorimetric assay for cellular growth and survival: Application to proliferation and cytotoxicity assays. J Immunol Methods. 1983;65(1-2):55-63. doi:10.1016/0022-1759(83)90303-4
[28] O'Brien J, Wilson I, Orton T, Pognan F. Investigation of the Alamar Blue (resazurin) fluorescent dye for the assessment of mammalian cell cytotoxicity. Eur J Biochem. 2000;267(17):5421-5426. doi:10.1046/j.1432-1327.2000.01606.x

[29] Riss TL, Moravec RA, Niles AL, et al. Cell viability assays. In: Sittampalam GS, Grossman A, Brimacombe K, et al., eds. Assay Guidance Manual. Eli Lilly & Company and the National Center for Advancing Translational Sciences; 2004.
[30] Mueller H, Kassack MU, Wiese M. Comparison of lactate dehydrogenase and MTT assays for anti-proliferative investigations on human carcinoma cells. Anticancer Res. 2004;24(4):2353-2363.
[31] Mithun TB, Anilakumar KR. Ethnopharmacology, phytochemistry and pharmacology of Syzygium cumini: A comprehensive review. Int J Pharm Pharm Sci. 2015;7(1):39-46.
[32] Kaufmann B, Christen P. Recent extraction techniques for natural products: microwave-assisted extraction and pressurised solvent extraction. Phytochem Anal. 2002;13(2):105-113. doi:10.1002/pca.631
[33] Prabhu P, Kurian R, Kumar DRA. Optimization and evaluation of phytochemical extraction using response surface methodology. Res J Pharm Technol. 2016;9(11):1931-1940.
[34] Edeoga HO, Okwu DE, Mbaebie BO. Phytochemical constituents of some Nigerian medicinal plants. Afr J Biotechnol. 2005;4(7):685-688. doi:10.5897/AJB2005.000-3127
[35] Tiwari P, Kumar B, Kaur M, Kaur G, Kaur H. Phytochemical screening and extraction: A review. Int Pharm Sci. 2011;1(1):98-106.
[36] Khandelwal KR. Practical Pharmacognosy: Techniques and Experiments. 19th ed. Nirali Prakashan; 2008.
[37] Trease GE, Evans WC. Pharmacognosy. 15th ed. W.B. Saunders; 1996.
[38] Harborne JB. Phytochemical Methods: A Guide to Modern Techniques of Plant Analysis. Chapman and Hall; 1998.
[39] Giusti MM, Wrolstad RE. Characterization and measurement of anthocyanins by UV-visible spectroscopy. In: Wrolstad RE, ed. Current Protocols in Food Analytical Chemistry. John Wiley & Sons; 2001. doi:10.1002/0471142913.fac0201s00
[40] Singleton VL, Rossi JA. Colorimetry of total phenolics with phosphomolybdic-phosphotungstic acid reagents. Am J Enol Viticult. 1965;16(3):144-158.
[41] Chang CC, Yang MH, Wen HM, Chern JC. Estimation of total flavonoid content in propolis by two complementary colorimetric methods. J Food Drug Anal. 2002;10(3):178-182. doi:10.38212/2224-6614.2748
[42] Lee J, Durst RW, Wrolstad RE. Determination of total monomeric anthocyanin pigment content of fruit juices, beverages, natural colorants, and dietary supplements by the pH differential method: Collaborative study. J AOAC Int. 2005;88(3):915-920. doi:10.1093/jaoac/88.3.915
[43] Sylvester PW. Optimization of the tetrazolium dye assay for screening plant extracts and fractions for antitumor and cytotoxic activities. In: Hostettmann K, ed. Methods in Molecular Medicine: Phytochemical Methods and Protocols. Humana Press; 1998:126-137.
[44] Sellins KS, Cohen JJ. Gene induction by gamma-irradiation leads to DNA fragmentation in lymphocytes. J Immunol. 1987;139(10):3199-3206.
[45] Wyllie AH, Morris RG, Smith AL, Dunlop D. Chromatin cleavage in apoptosis: Association with condensed chromatin morphology and dependence on macromolecular synthesis. J Pathol. 1984;142(1):67-77. doi:10.1002/path.1711420109
[46] Brand-Williams W, Cuvelier ME, Berset C. Use of a free radical method to evaluate antioxidant activity. Lebensm Wiss Technol. 1995;28(1):25-30. doi:10.1016/S0023-6438(95)80008-5
[47] Mushtaq M, Sultana B, Bhatti IA, Anwar F. Enzyme-assisted and ultrasound extraction of antioxidative compounds from pomegranate (Punica granatum L.) peel. Food Hydrocoll. 2015;46:157-164. doi:10.1016/j.foodhyd.2014.12.039
[48] Aziz N, Kim MY, Cho JY. Anti-inflammatory effects of luteolin: Isolation from rapeseed sprouts and suppression of pro-inflammatory cytokines by inhibiting NF-κB activation in macrophages. Inflammation. 2018;41(1):229-237. doi:10.1007/s10753-017-0680-8
[49] Neubig RR, Spedding M, Kenakin T, Christopoulos A. International Union of Pharmacology Committee on Receptor Nomenclature and Drug Classification. XXXVIII. Update on terms and symbols in quantitative pharmacology. Pharmacol Rev. 2003;55(4):597-606. doi:10.1124/pr.55.4.4
[50] Raji Y, Faloye SK, Olurinde MO, Dada SA. Cytotoxic and apoptosis-inducing activity of Azadirachta indica leaf extract against human lung carcinoma A549 cells. Pharm Biol. 2019;57(1):246-254. doi:10.1080/13880209.2019.1606380
[51] Sa G, Das T. Anti cancer effects of curcumin: cycle arrest and apoptosis. Curr Mol Med. 2008;8(7):649-667. doi:10.2174/156652408786241375
[52] Wang X, Zhang W, Zhao Y. Antitumor effects of EGCG on human lung cancer A549 cells through apoptosis and G0/G1 phase arrest. Cell Biol Int. 2018;42(12):1664-1673. doi:10.1002/cbin.11070
[53] Lim TG, Lim DY, Gerhauser C, et al. Xanthohumol induces growth inhibition and apoptosis in insect cells and human cancer cells. Mol Carcinog. 2012;51(8):618-628. doi:10.1002/mc.20829

[54] Fithrotunnisa Q, Andarini S, Sugiyanto A, et al. In vitro cytotoxicity of Hibiscus sabdariffa Linn extract on A549 human lung cancer cell line. Phcog J. 2020;12(1):47-57. doi:10.5530/pj.2020.12.8
[55] Malik F, Singh J, Khajuria A, et al. A standardized root extract of Withania somnifera and its major constituent withanolides enhance cytokine production and immune responses in diseased conditions. J Ethnopharmacol. 2009;123(3):510-517. doi:10.1016/j.jep.2009.03.012
[56] Carvalho C, Santos RX, Cardoso S, et al. Doxorubicin: the good, the bad and the ugly effect. Curr Med Chem. 2009;16(25):3267-3285. doi:10.2174/092986709788803312
[57] Gopal J, Muthu M, Paul V, Chun SS. Phytochemical distribution and cytotoxic evaluation of Portulaca oleracea extract fractions. Braz J Pharmacogn. 2016;26(2):234-240. doi:10.1016/j.bjp.2015.10.005
[58] Losso JN, Bansode RR, Trappey A, Bawadi HA, Truax R. In vitro anti-proliferative activities of ellagic acid. J NutrBiochem. 2004;15(11):672-678. doi:10.1016/j.jnutbio.2004.05.007
[59] Hamsa TP, Kuttan G. Antiangiogenic activity of ursolic acid. Integr Cancer Ther. 2010;9(2):224-235. doi:10.1177/1534735410370210
[60] Leopoldini M, Russo N, Chiodo S. The molecular basis of working mechanism of natural polyphenolic antioxidants. Food Chem. 2011;125(2):288-306. doi:10.1016/j.foodchem.2010.08.012
[61] Christopoulos A. Advances in G-protein-coupled receptor pharmacology. Golden Bullets to target obesity and diabetes. Front Endocrinol. 2014;5:214. doi:10.3389/fendo.2014.00214
[62] Green DR, Kroemer G. The pathophysiology of mitochondrial cell death. Science. 2004;305(5684):626-629. doi:10.1126/science.1099320
[63] Rahman I, Biswas SK, Kode A. Oxidative stress and airway inflammation in COPD. Eur Respir J. 2006;28(10):219-242. doi:10.1183/09031936.06.00053805
[64] Gogvadze V, Orrenius S, Zhivotovsky B. Mitochondrial control of apoptosis: an update. Apoptosis. 2006;11(5):803-809. doi:10.1007/s10495-006-5761-5
[65] Danial NN, Korsmeyer SJ. Cell death: critical control points. Cell. 2004;116(2):205-219. doi:10.1016/S0092-8674(04)00046-7
[66] Hill MM, Adrain C, Duriez PJ, Creagh EM, Martin SJ. Analysis of the composition, assembly kinetics and activity of native Apaf-1 apoptosomes. EMBO J. 2004;23(10):2134-2145. doi:10.1038/sj.emboj.7600213
[67] Pop C, Salvesen GS. Human caspases: activation, specificity, and regulation. J Biol Chem. 2009;284(33):21777-21781. doi:10.1074/jbc.R800084200
[68] Slee EA, Harte MT, Kluck RM, et al. Ordering the cytochrome c-initiated caspase cascade: hierarchical activation of caspases-2, -3, -6, -7, -8, and -10 in a caspase-9-dependent manner. J Cell Biol. 1999;144(2):281-292. doi:10.1083/jcb.144.2.281
[69] Kerr JF, Wyllie AH, Currie AR. Apoptosis: a basic biological phenomenon with wide-ranging implications in tissue kinetics. Br J Cancer. 1972;26(4):239-257. doi:10.1038/bjc.1972.33
[70] Hollstein M, Sidransky D, Vogelstein B, Harris CC. p53 mutations in human cancers. Science. 1991;253(5015):49-53. doi:10.1126/science.1905840
[71] Abraham RT. Cell cycle checkpoint signaling through the ATM and ATR kinases. Genes Dev. 2001;15(17):2177-2196. doi:10.1101/gad.914401
[72] Seabra AB, Justo GZ, Haddad PS. State-of-the-art, challenges and perspectives in the design of polyphenol-nanostructure interactions for targeted drug delivery and synergism in phytomedicine. Molecules. 2018;23(12):3387. doi:10.3390/molecules23123387
[73] Slee EA, O'Neill JK, Fay E, Higgins M, Mati-Bouzid S, Martin SJ. Morphological and biochemical analysis of apoptosis in L929 fibroblasts following growth factor deprivation. Eur J Cell Biol. 1999;78(7):479-488. doi:10.1016/S0171-9335(99)80050-9
[74] Leopoldini M, Russo N, Chiodo S. The molecular basis of working mechanism of natural polyphenolic antioxidants. Food Chem. 2011;125(2):288-306. doi:10.1016/j.foodchem.2010.08.012
[75] Mattson MP. Hormesis and disease resistance: activation of cellular stress response pathways. Hum Exp Toxicol. 2008;27(2):155-162. doi:10.1177/0960327107083174
[76] Aaby K, Ekeberg D, Skrede G. Phenolic compounds in plant extracts of Japanese medlar (Eriobotrya japonica), quince (Cydonia oblonga), and related Mespilus species. J Agric Food Chem. 2005;53(3):592-598. doi:10.1021/jf048926+
[77] Trachootham D, Alexandre J, Huang P. Targeting cancer cells by ROS-mediated mechanisms: a radical therapeutic approach? Nat Rev Drug Discov. 2009;8(7):579-591. doi:10.1038/nrd2803

[78] Carvalho C, Santos RX, Cardoso S, et al. Doxorubicin: the good, the bad and the ugly effect. Curr Med Chem. 2009;16(25):3267-3285. doi:10.2174/092986709788803312
[79] Liang Y, Yan W, Ding Y, Ren X, Xu L, Liang L. Characterizing the cellular miRNA-mRNA regulatory network for different stages of breast cancer progression. Oncol Rep. 2016;36(5):2843-2852. doi:10.3892/or.2016.5101
[80] Kinghorn AD, Pan L, Fletcher JN, Chai H. The relevance of higher plants in lead compound discovery programs. J Nat Prod. 2011;74(6):1539-1555. doi:10.1021/np200040x
[81] Duval K, Grover H, Han LH, et al. Modeling physiological events in 2D vs. 3D cell culture. Physiology. 2017;32(4):266-277. doi:10.1152/physiol.00036.2016

How to cite this article:
Shrasti Singh et al. Ijppr.Human, 2026; Vol. 32 (4): 325-340.
Conflict of Interest Statement: All authors have nothing else to disclose.